

# Hydrothermal synthesis of $\text{KNbO}_3$ and $\text{NaNbO}_3$ powders

Gregory K.L. Goh<sup>a)</sup> and Fred F. Lange

Materials Department and Materials Research Laboratory, University of California,  
Santa Barbara, California 93106

Sossina M. Haile

Materials Science Department 138-78, California Institute of Technology, 1200 California Boulevard,  
Pasadena, California 91125

Carlos G. Levi

Materials Department and Materials Research Laboratory, University of California,  
Santa Barbara, California 93106

(Received 22 July 2002; accepted 28 October 2002)

Orthorhombic  $\text{KNbO}_3$  and  $\text{NaNbO}_3$  powders were hydrothermally synthesized in KOH and NaOH solutions (6.7–15 M) at 150 and 200 °C. An intermediate hexaniobate species formed first before eventually converting to the perovskite phase. For synthesis in KOH solutions, the stability of the intermediate hexaniobate ion increased with decreasing KOH concentrations and temperatures. This led to significant variations in the induction periods and accounted for the large disparity in the mass of recovered powder for different processing parameters. It is also believed that protons were incorporated in the lattice of the as-synthesized  $\text{KNbO}_3$  powders as water molecules and hydroxyl ions.

## I. INTRODUCTION

$\text{KNbO}_3$  is a promising material for electro-optic, non-linear optical, and photorefractive applications such as frequency doubling, wave guiding, and holographic storage.<sup>1–3</sup> In conventional, solid-state synthesis of  $\text{KNbO}_3$  using mixed powders, prolonged heating at a high temperature (820 °C) is required.<sup>4</sup> More recently,  $\text{KNbO}_3$  has been synthesized by the sol-gel method in which alkoxide precursors are used to produce an amorphous gel that is calcined at 600 °C to remove the organic components of the gel and to yield crystalline  $\text{KNbO}_3$ .<sup>5,6</sup> An aqueous solution route has also been used to precipitate amorphous  $\text{KNbO}_3$  powders at 25 °C, which is then crystallized by heating to 600 °C.<sup>7</sup> In contrast, crystalline  $\text{KNbO}_3$  powders can be synthesized by the hydrothermal method at temperatures below 200 °C.<sup>8,9</sup>

Unlike  $\text{BaTiO}_3$ , the hydrothermal synthesis of  $\text{KNbO}_3$  powders has not been extensively investigated. Komarneni and co-workers<sup>8</sup> reported that  $\text{KNbO}_3$  could be synthesized at 194 °C by reacting  $\text{Nb}_2\text{O}_5$  in a solution containing 3 M  $\text{OH}^-$  and 9 M  $\text{K}^+$  while Uchida *et al.*<sup>10</sup> reported using 3 M KOH at 250 °C. Lu *et al.* obtained

orthorhombic  $\text{KNbO}_3$  (the stable form) by reacting  $\text{Nb}_2\text{O}_5$  with 8 M KOH at 200 °C and observed that the crystal structure became cubic with increasing niobium concentration in the solution.<sup>9</sup> Both Komarneni *et al.*<sup>8</sup> and Lu *et al.*<sup>9</sup> noticed large variations in the amount of powder recovered for different KOH concentrations. Lu *et al.*<sup>9</sup> qualitatively described the amount of recovered powder with terms such as a large amount when using 8 M KOH, a small amount when using 6 M KOH, and no precipitates when 4 M KOH was used. (The comparisons were made for synthesis at 200 °C after 2 h with 0.1 M of  $\text{Nb}_2\text{O}_5$  powder.)

$\text{NaNbO}_3$  is antiferroelectric at room temperature. This lack of spontaneous polarization at room temperature accounts for the comparatively lower interest in  $\text{NaNbO}_3$  than in  $\text{KNbO}_3$ .  $\text{NaNbO}_3$  does, however, form a solid solution with  $\text{KNbO}_3$  that is ferroelectric at room temperature and has recently attracted attention as a promising component for nonvolatile memory devices, actuators, and microsensors.<sup>11,12</sup>

Although  $\text{NaNbO}_3$  powders are also synthesized in this study, the main focus is on hydrothermally synthesized  $\text{KNbO}_3$ . One issue addressed is the variation in the amount of reaction products often recovered in the hydrothermal synthesis of  $\text{KNbO}_3$  powder, as mentioned earlier. Another issue concerns the defect structure of the as-synthesized  $\text{KNbO}_3$  powder and the role that protons play in this structure.

<sup>a)</sup>Address all correspondence to this author.

Present address: Institute of Materials Research and Engineering,  
3 Research Link, Singapore 117602, Republic of Singapore.  
e-mail: g-goh@imre.org.sg

## II. EXPERIMENTAL

NaNbO<sub>3</sub> powders were synthesized by reacting 2 g Nb<sub>2</sub>O<sub>5</sub> powder with 30 ml aqueous solutions (resulting in an Nb<sub>2</sub>O<sub>5</sub> concentration of 0.25 M) of 8.4 M NaOH at 200 °C. KNbO<sub>3</sub> powder syntheses were performed for the following reaction conditions: 6.7 M KOH/0.15 M Nb<sub>2</sub>O<sub>5</sub>/200 °C, 6.7 M KOH/0.25 M Nb<sub>2</sub>O<sub>5</sub>/150 °C, and 9 M KOH/0.38 M Nb<sub>2</sub>O<sub>5</sub>/200 °C. Alkaline solutions were made from NaOH (99%, Merck, Darmstadt, Germany) or KOH (86–89%, Merck) pellets (<0.5% carbonates). KNbO<sub>3</sub> powder was also synthesized at 150 °C in 15 M KOH precursor solutions containing 0.0015 M of predissolved Nb<sub>2</sub>O<sub>5</sub> powder. (Details on the preparation of the precursor solution containing predissolved Nb<sub>2</sub>O<sub>5</sub> will be given in Sec. III. B.)

Nb<sub>2</sub>O<sub>5</sub> has a large variety of polymorphs that are referred to as TT-, T-, B-, N-, P-, M-, and H-Nb<sub>2</sub>O<sub>5</sub>.<sup>13</sup> Under ambient conditions, H-Nb<sub>2</sub>O<sub>5</sub> is the only stable form.<sup>14</sup> The Nb<sub>2</sub>O<sub>5</sub> powder supplied (99.99%, Aldrich, Milwaukee, WI) was composed of two modifications; T- and H-Nb<sub>2</sub>O<sub>5</sub>. Some batches consisted mainly of T-Nb<sub>2</sub>O<sub>5</sub>,<sup>15</sup> while other batches were a mixture of the T and H forms. All syntheses, except for the 15 M KOH condition, which used T-Nb<sub>2</sub>O<sub>5</sub> powder, were performed using the H+T Nb<sub>2</sub>O<sub>5</sub> powder. The reactions were carried out unstirred in a 45 ml Teflon-lined stainless steel bomb (Parr Co., Moline, IL) for periods ranging from 30 min to 143 h. After reaction, the solutions were separated from the powders, and the powders were centrifuge-washed with deionized water and dried at 100 °C.

Raman spectroscopy (Magna IR 850 Series II, Nicolet, Madison, WI) was used to examine an intermediate complex that resulted from some experiments. To probe the chemical environment of the Nb ions in the synthesis environment, solution <sup>93</sup>Nb nuclear magnetic resonance (NMR) spectroscopy was performed on an AVANCE500 spectrometer (Bruker, Rheinstetten, Germany) at room temperature (25 °C). The spectra were referenced to an external 0.25 M solution of NbCl<sub>5</sub> in CD<sub>3</sub>CN (Wilma Labglass, Buena, NJ).

The morphology of the resultant powders was examined by field emission scanning electron microscopy (FE-SEM; 6300F, JEOL Ltd., Tokyo, Japan) and by powder transmission electron microscopy (TEM; JEOL 2000FX, JEOL Ltd.). Compositional analysis was performed by energy dispersive spectroscopy (EDS; Oxford Instruments, Oxford, U.K.). Phase identification was carried out by x-ray diffraction (XRD; Philips X'pert, Philips, Mahwah, NJ).

The presence of water in the powders was determined by Fourier-transform infrared (FTIR) spectroscopy (Magna IR 850 Series II, Nicolet, Madison, WI). Powders were diluted to about 1 wt% with KBr and heated at 130 °C in a vacuum oven for at least 4 h to remove excess

surface water before analysis in dry nitrogen. Each spectrum collected (400–4000 cm<sup>-1</sup>) was the average of 64 measurements with a 4 cm<sup>-1</sup> resolution. The presence of protons in the KNbO<sub>3</sub> powders synthesized in 6.7 M KOH was confirmed by <sup>1</sup>H magic-angle spinning nuclear magnetic resonance (MAS NMR, 12 kHz spinning rate) on a DSX 500 spectrometer (Bruker) at room temperature (25 °C) with an external tetramethylsilane reference. The water content of the powders was quantified by thermogravimetric analyses (TGA; TGA/sDTA 851e, Mettler, Toledo, OH) coupled with mass spectrometry (ThermoStar, Pfeiffer Vacuum, Nashua, NH). The TGA was performed at a heating rate of 10 °C/min from 25 to 900 °C in a dry nitrogen atmosphere.

## III. RESULTS

### A. Synthesis of NaNbO<sub>3</sub> and KNbO<sub>3</sub> powders

XRD of NaNbO<sub>3</sub> powders hydrothermally synthesized at 200 °C in 8.4 M NaOH/0.25 M Nb<sub>2</sub>O<sub>5</sub> (H+T form) in this study indicated that an intermediate, sodium hexaniobate (Na<sub>8</sub>Nb<sub>6</sub>O<sub>19</sub> · 13H<sub>2</sub>O),<sup>16</sup> formed during the initial synthesis stages and then finally converted to the orthorhombic perovskite structure of NaNbO<sub>3</sub>.<sup>17</sup> In contrast, XRD of powders recovered from synthesis in KOH solutions did not show the presence of a potassium hexaniobate.

For KNbO<sub>3</sub> powders synthesized in 6.7 M KOH/0.15 M Nb<sub>2</sub>O<sub>5</sub> (H+T form) at 200 °C, diffraction patterns for several different reaction periods are presented in Fig. 1. The results show that after 2 h, the diffraction peaks belonging to T-Nb<sub>2</sub>O<sub>5</sub> were no longer present. After 4 h, the powder consisted mainly of KNbO<sub>3</sub>, with some

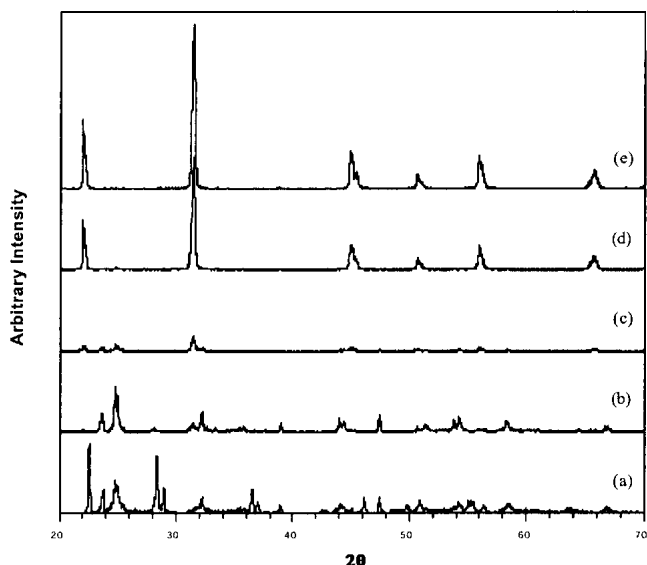


FIG. 1. (a) XRD pattern of Nb<sub>2</sub>O<sub>5</sub> powder and of products obtained from synthesis at 200 °C in 6.7 M KOH/0.15 M Nb<sub>2</sub>O<sub>5</sub> solution, and after (b) 2 h, (c) 3 h, (d) 4 h, and (e) 8 h.

H-Nb<sub>2</sub>O<sub>5</sub> still present; only the KNbO<sub>3</sub> phase was present at 8 h and beyond. Comparison of the XRD pattern of the KNbO<sub>3</sub> powder obtained after 16 h with information in literature<sup>18</sup> results revealed that the hydrothermally synthesized powder had an orthorhombic structure, the thermodynamically stable structure at room temperature.<sup>19</sup> The K/Nb ratio was determined by EDS to be 0.96.

SEM [Fig. 2(a)] revealed that the KNbO<sub>3</sub> powder produced after 16 h consisted of particles ranging from 100 to 500 nm in size. All particles were bound by flat faces that appeared to be orthogonal to each other. Figure 2(b) is a TEM micrograph of a particle with well-developed facets; the corresponding selected area diffraction pattern [Fig. 2(c)] shows that it is a single crystal. TEM observations further revealed that the facets were the {100}<sub>pc</sub> planes (pc = pseudo-cubic),<sup>19</sup> as has been observed for bulk KNbO<sub>3</sub> single crystals grown from the melt.<sup>20</sup>

As for KNbO<sub>3</sub> powder synthesized at 150 °C in 15 M KOH using 0.0015 M predissolved Nb<sub>2</sub>O<sub>5</sub>, XRD of particles produced after 16 h [Fig. 3(a)] suggested that the KNbO<sub>3</sub> powder had a metastable cubic structure, similar to that reported for KNbO<sub>3</sub> powders hydrothermally synthesized at 200 °C in 8 M KOH after 2 h.<sup>9</sup> However, XRD scans at higher 2θ values revealed that the (004) peak was split [Fig. 3(b)] and that the powder was probably orthorhombic, similar to that observed for the powder synthesized in 6.7 M KOH. The K/Nb ratio determined by EDS was 0.94. Observations of the powders synthesized after 8 and 16 h by SEM showed that the particle shape was rather anisotropic with towerlike structures growing from cube-shaped cores, as shown for the 8 h particles in Fig. 4. Details relating to the towerlike structures will be presented in a separate study on the hydrothermal synthesis of epitaxial KNbO<sub>3</sub> films.<sup>21</sup>

## B. Hexaniobate ion

Figure 5 shows the change in the normalized mass of KNbO<sub>3</sub> and NaNbO<sub>3</sub> powders with processing time for several processing conditions. The normalized mass is the mass of recovered powder normalized to the maximum yield of perovskite powder possible for the given amount of Nb<sub>2</sub>O<sub>5</sub> powder used. When NaOH was used, the normalized mass was greater than one when Na<sub>8</sub>Nb<sub>6</sub>O<sub>19</sub> · 13H<sub>2</sub>O was present (<2 h), since its

molecular weight is greater than that of NaNbO<sub>3</sub>. For the reaction in 6.7 M KOH/0.15M Nb<sub>2</sub>O<sub>5</sub> at 200 °C, the normalized mass decreased rapidly within the first 2 h of the reaction and remained low before a sharp increase

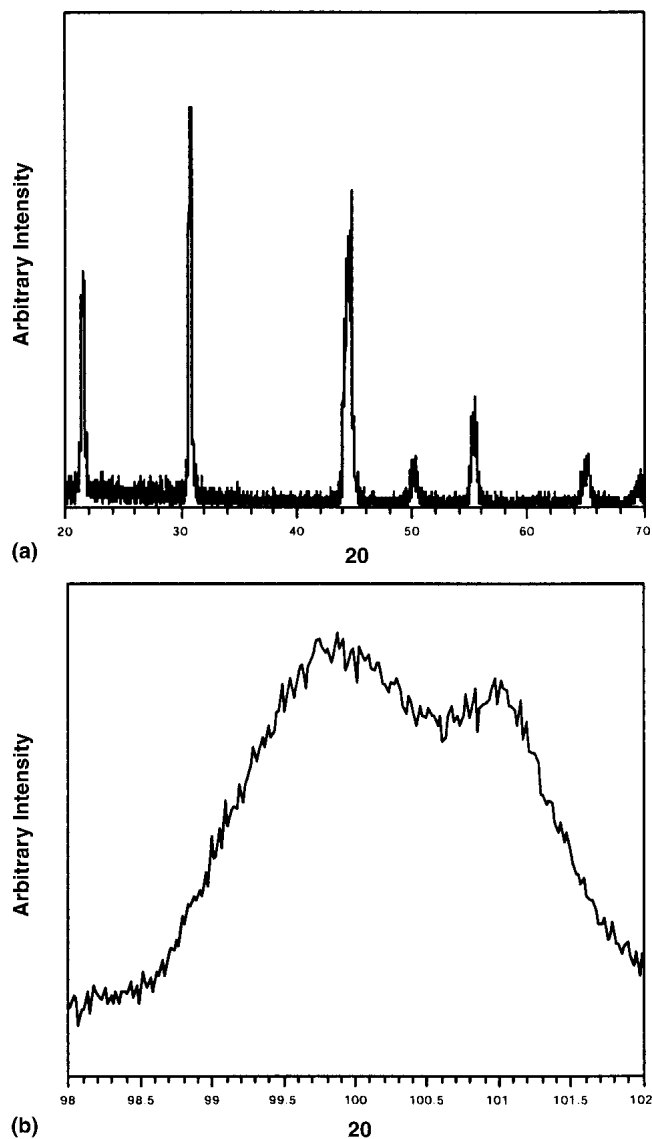


FIG. 3. XRD of KNbO<sub>3</sub> powder produced after 16 h at 150 °C from 15 M KOH/0.0015 M Nb<sub>2</sub>O<sub>5</sub> solution for (a) 2θ = 20° to 70° and (b) 2θ = 98° to 102°.

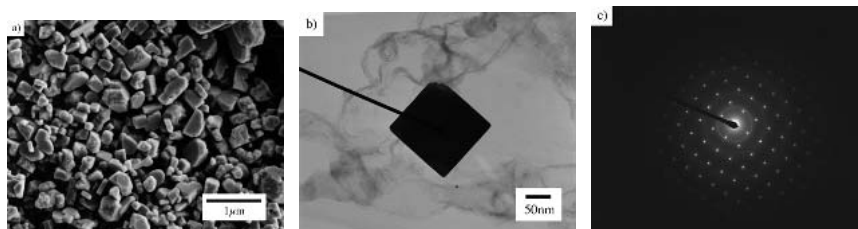


FIG. 2. KNbO<sub>3</sub> powder produced after 16 h at 200 °C from 6.7 M KOH/0.15 M Nb<sub>2</sub>O<sub>5</sub> solution: (a) SEM micrograph, (b) TEM micrograph of a particle, and (c) selected area diffraction pattern of particle in (b) in [001] zone axis.

between 6 and 8 h. This induction period was shorter for powders synthesized at 9 M KOH/0.38 M Nb<sub>2</sub>O<sub>5</sub>/200 °C but longer for powders synthesized at 6.7 M KOH/0.25 M Nb<sub>2</sub>O<sub>5</sub>/150 °C.

For solutions obtained during the induction period for synthesis in KOH, it was noticed that transparent and colorless crystals precipitated out of the solution several hours after the solution had cooled down to room temperature. Raman spectroscopy of these crystals while they were still in the parent solution indicated the presence of the hexaniobate ion, Nb<sub>6</sub>O<sub>19</sub><sup>8-</sup>.<sup>22,23</sup> The peak positions observed for crystals in 6.7 M KOH/0.15 M Nb<sub>2</sub>O<sub>5</sub> solutions are summarized in Table I.

For KNbO<sub>3</sub> powders synthesized at 15 M KOH, T-Nb<sub>2</sub>O<sub>5</sub> was first completely dissolved in 4 M KOH by heating at 200 °C for 16 h in the bomb. The resultant clear solution was then added to a KOH solution through a 0.20- $\mu$ m syringe filter (Cole-Parmer, Vernon Hills, IL) to give a final KOH concentration of 15 M. The use of

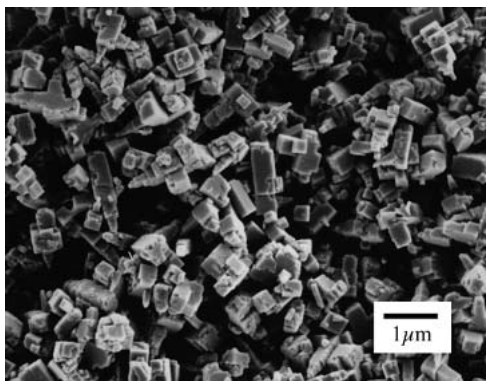


FIG. 4. SEM of KNbO<sub>3</sub> powder produced after 16 h at 150 °C from 15 M KOH/0.0015 M Nb<sub>2</sub>O<sub>5</sub> solution.

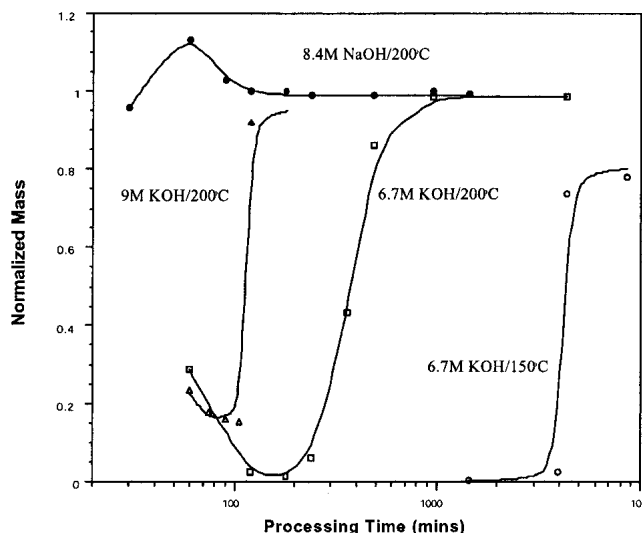


FIG. 5. Variation of normalized mass as a function of time for KNbO<sub>3</sub> (open symbols) and NaNbO<sub>3</sub> (closed symbols) powders.

predissolved Nb<sub>2</sub>O<sub>5</sub> precursor solutions was done to confirm if the perovskite phase could be formed from the reaction of the hexaniobate species with KOH. The concentration 15 M is also of interest in the hydrothermal synthesis of epitaxial KNbO<sub>3</sub> films using predissolved Nb<sub>2</sub>O<sub>5</sub>, details of which will be reported in a separate study.<sup>21</sup>

Attempts to make a 0.15 M Nb<sub>2</sub>O<sub>5</sub> solution always led to the precipitation of potassium hexaniobate particles, as determined by Raman spectroscopy (the peak positions are reported in Table I). To prepare clear 15 M KOH/Nb<sub>2</sub>O<sub>5</sub> precursor solutions, a Nb<sub>2</sub>O<sub>5</sub> concentration of 0.0015 M was used. For such a solution, Raman spectroscopy revealed only peaks characteristic of the KOH solution and none belonging to the hexaniobate ion, probably due to the greatly reduced concentration of Nb<sub>2</sub>O<sub>5</sub>. <sup>93</sup>Nb NMR spectroscopy was therefore used to determine the presence of the hexaniobate ion in the solution.

Figure 6(a) shows the spectrum for the reference solution of NbCl<sub>5</sub> in CD<sub>3</sub>CN. In addition to the NbCl<sub>5</sub> peak, there was also a sharp peak at  $\delta = 54$  due to NbCl<sub>6</sub><sup>-</sup>, which indicated that strictly anhydrous conditions were not maintained in the production of the reference solution.<sup>24</sup> As shown in Fig. 6(b), the spectrum for the hexaniobate ion (as determined earlier by Raman spectroscopy) in a 15 M KOH solution containing 0.15 M Nb<sub>2</sub>O<sub>5</sub> showed only one extremely broad resonance at -280 ppm with  $W_{1/2} = 31$  kHz. A single, similarly broad resonance was also seen at -307 ppm for the 6.7 M KOH/0.15 M Nb<sub>2</sub>O<sub>5</sub>/200 °C solution and at -297 ppm for the 15 M KOH/0.0015 M Nb<sub>2</sub>O<sub>5</sub> solution.

### C. Proton incorporation

Figure 7 shows the room-temperature FTIR spectra of KNbO<sub>3</sub> powder synthesized at 150 °C from 15 M KOH/0.0015 M Nb<sub>2</sub>O<sub>5</sub> precursor solutions, hereafter referred to as the 15 M powder. The broad band from 3000 to 3600 cm<sup>-1</sup> is due to overlapping O-H stretching vibrations of H<sub>2</sub>O and hydroxyl ions while the peak at 1600–1650 cm<sup>-1</sup> is due to the bending vibration of H<sub>2</sub>O.<sup>25</sup> The KNbO<sub>3</sub> powder synthesized at 200 °C in 6.7 M KOH/0.15 M Nb<sub>2</sub>O<sub>5</sub> (hereafter referred to as the 6.7 M powder) displayed a similar spectrum except for the absence of the sharp peak at 3637 cm<sup>-1</sup> in the 15 M spectra attributed to the presence of free hydroxyls.<sup>26,27</sup> As far as the authors are aware, a free hydroxyl peak has never been reported for hydrothermally synthesized perovskite powders.

TABLE I. Peak positions from Raman spectra of hexaniobate particles in KOH/0.15M Nb<sub>2</sub>O<sub>5</sub> parent solutions.

[KOH]	Wave number (cm <sup>-1</sup> )
6.7 M	866, 812, 740, 529, 453, 299, 224
15 M	885, 825, 741, 541, 500, 292, 259, 240, 223

TGA of the 6.7 M and 15 M powders revealed total weight losses of 0.98 and 1.13 wt%, respectively. Concurrent mass spectrometry indicated that these weight losses were associated with the evolution of water. It was also observed that 38% and 74% of these losses occurred at temperatures lower than 350 °C for the 6.7 M and 15 M powders, respectively, as illustrated in Fig. 8 for the 6.7 M powder. The TGA curve for the 15 M powder had a similar profile.

<sup>1</sup>H MAS NMR was also carried out on the 6.7 M powder. As shown in Fig. 9, there are two groups of peaks. The group with the higher intensity was found to be composed of two peaks at 4.95 and 4.44 ppm, shifts that are probably more typical of internally incorporated protons with OH<sup>-</sup> stretching frequencies around 3400 cm<sup>-1</sup>.<sup>28</sup> The other group consisted of four peaks with shifts ranging from 0.84 to 1.74 ppm; the peaks were

much sharper. These peaks were probably due to surface H<sub>2</sub>O or surface hydroxyl groups. The integrated <sup>1</sup>H MAS NMR signal for the two peaks at 4.95 and 4.44 ppm is 91% of the total value for all the peaks, indicating that 91% of the protons were internally incorporated. Accordingly, this means that the weight loss due to internally incorporated protons for the 6.7 M powder is 0.89 wt%.

## IV. DISCUSSION

### A. Hexaniobate ion

The hexaniobate ion is composed of six edge-sharing NbO<sub>6</sub> octahedra, forming a super-octahedron, as shown in Fig. 10(a). As confirmed by <sup>17</sup>O NMR spectroscopy,<sup>29</sup>

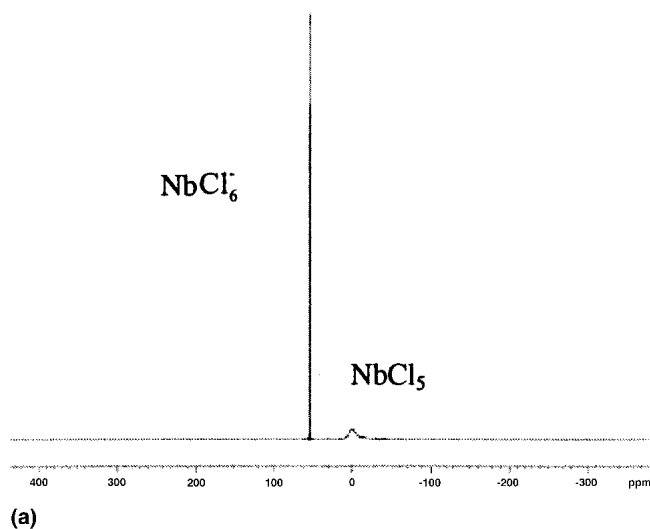


FIG. 6. Room-temperature <sup>93</sup>Nb solution NMR spectra of (a) 0.25 M NbCl<sub>5</sub> reference solution and (b) 15 M KOH/0.15 M Nb<sub>2</sub>O<sub>5</sub> precursor solution.

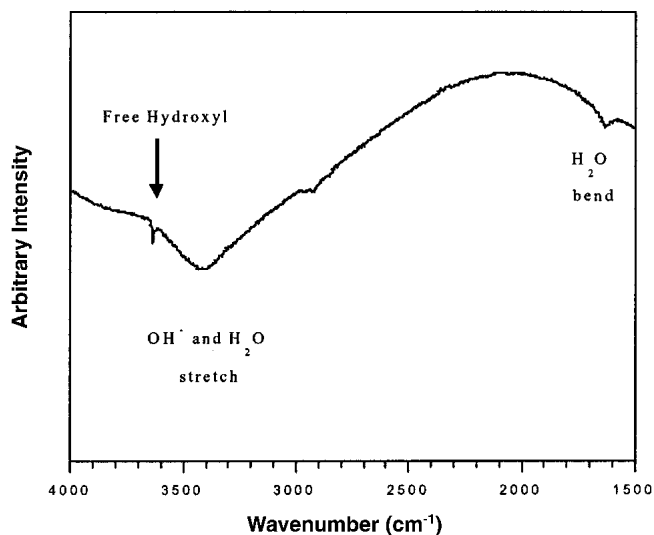


FIG. 7. FTIR spectra of KNbO<sub>3</sub> powder produced after 16 h at 150 °C from 15 M KOH/0.0015 M Nb<sub>2</sub>O<sub>5</sub> solution.

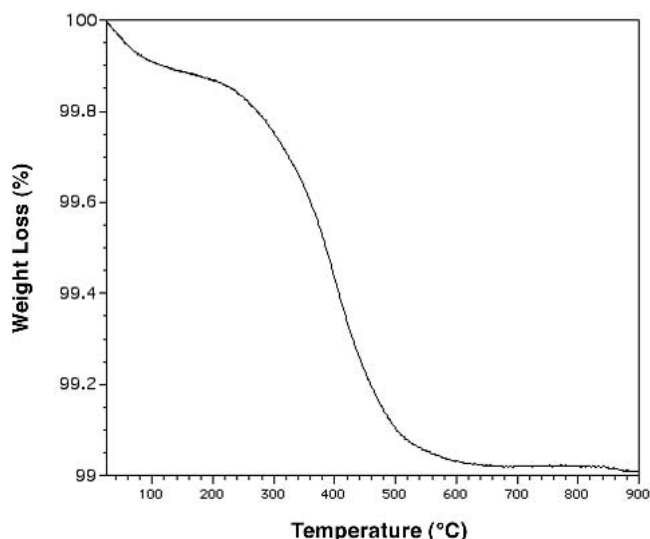


FIG. 8. TGA curve of KNbO<sub>3</sub> powder produced after 16 h at 200 °C from 6.7 M KOH/0.15 M Nb<sub>2</sub>O<sub>5</sub> solution.

this arrangement gives rise to three different types of oxygen atoms; 6 terminal (O<sub>t</sub>), 12 bridging (O<sub>b</sub>), and 1 central (O<sub>c</sub>). The unfavorable niobium–niobium electrostatic repulsions resulting from this arrangement are accommodated by distortion of the NbO<sub>6</sub> octahedra [Fig. 10(b)].<sup>30</sup> It has been shown by Raman spectroscopy that the structure of the hexaniobate unit in the crystalline state is retained in aqueous solution.<sup>22</sup> The strong inward polarization of the exterior layer of oxygens (O<sub>t</sub>) hinders polymerization and is the reason why the apparently highly charged complex can exist as discrete species in solution.<sup>31</sup> Protonation of the complex to form H<sub>x</sub>Nb<sub>6</sub>O<sub>19</sub><sup>8-x</sup> ( $x = 1$  to 3) is generally observed only below pH 14.<sup>32</sup>

The band positions in the Raman spectra of the hexaniobate ion have previously been assigned as follows:<sup>33</sup> Nb–O<sub>t</sub> stretching in the 800 to 900 cm<sup>-1</sup> range, edge-shared NbO<sub>6</sub> octahedra stretching in the 800 to 400 cm<sup>-1</sup> range, Nb–O<sub>c</sub> stretching around 290 cm<sup>-1</sup>, and Nb–O<sub>b</sub>–Nb bending around 230 cm<sup>-1</sup>. Thus the difference in band positions of the hexaniobate ion in 6.7 M and 15 M KOH (see Table I) indicates that the bond lengths and angles are not the same. This agrees with <sup>93</sup>Nb NMR observations that the resonance positions, which are sensitive to the bonding environment of the niobium ion, are also not the same.

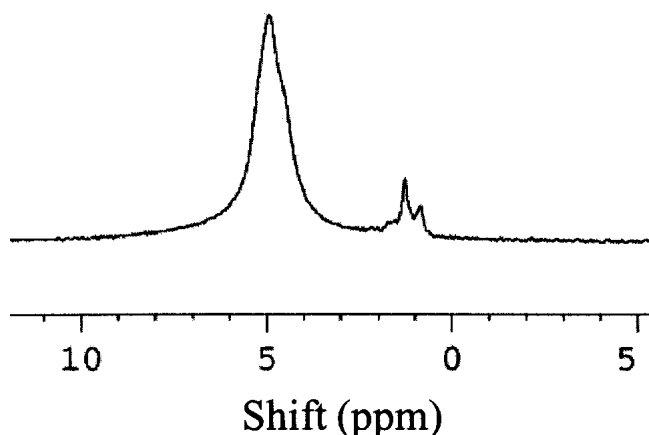


FIG. 9. <sup>1</sup>H NMR spectra for KNbO<sub>3</sub> powder produce after 16 h at 200 °C from 6.7 M KOH/0.15 M Nb<sub>2</sub>O<sub>5</sub> solution.

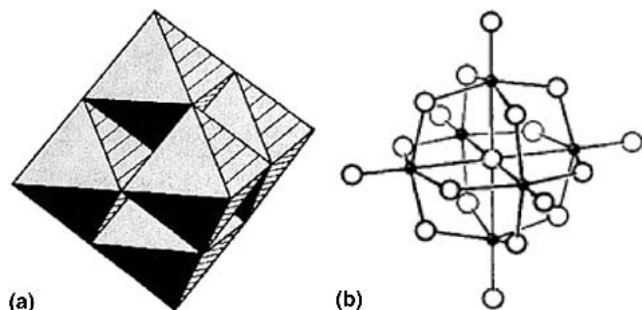


FIG. 10. Structure of hexaniobate ion, Nb<sub>6</sub>O<sub>19</sub><sup>8-</sup>: (a) edge sharing NbO<sub>6</sub> octahedra model and (b) bond length model (after Ref. 30).

It has been proposed, on the basis of ultraviolet and Raman spectroscopy, that it is the tetrameric, Nb<sub>4</sub>O<sub>12</sub>(OH)<sub>4</sub><sup>8-</sup>, and monomeric, NbO<sub>2</sub>(OH)<sub>4</sub><sup>3-</sup>, forms that are present in highly concentrated (6–12 M) KOH solutions instead of the hexamer.<sup>34,35</sup> This is in contrast to Griffith and Wickins, who observed only Raman bands typical of the hexaniobate ion in a 12 M KOH solution.<sup>36</sup> The presence of the hexaniobate ion at high KOH concentrations (6.7 and 15 M) was also observed in this study, as confirmed by Raman spectroscopy. In addition, as detailed below, the absence of the monomer in 6.7 and 15 M KOH solutions at room temperature was also confirmed by solution <sup>93</sup>Nb NMR spectroscopy.

The large quadrupolar moment of the Nb nucleus often results in broad NMR resonances.<sup>37</sup> In addition, the number and arrangement of Nb nuclei with respect to each other has been observed to affect the line width  $W_{1/2}$  of <sup>93</sup>Nb NMR resonances. For example, [(C<sub>4</sub>H<sub>9</sub>)<sub>4</sub>N]<sub>3</sub>NbW<sub>5</sub>O<sub>19</sub>, which has a super-octahedron composed of five WO<sub>6</sub> and one NbO<sub>6</sub> octahedra all sharing edges, has a  $W_{1/2}$  of 900 Hz. When condensation occurs to form [(C<sub>4</sub>H<sub>9</sub>)<sub>4</sub>N]<sub>4</sub>(NbW<sub>5</sub>O<sub>18</sub>)<sub>2</sub>O by corner sharing of the NbO<sub>6</sub> octahedra via its terminal oxygen,  $W_{1/2}$  increases to 6000 Hz.<sup>38</sup> A  $W_{1/2}$  of 21,000 Hz has been observed for [Nb(μ-OEt)(ONp)<sub>4</sub>]<sub>2</sub> in which two NbO<sub>6</sub> octahedra share edges.<sup>24</sup> In general, these observations indicate that isolated, monomeric Nb units lead to sharp peaks, whereas broad peaks result from units containing several Nb atoms in close proximity. The absence of a sharp resonance in the <sup>93</sup>Nb NMR spectra for the 6.7 and 15 M KOH solutions in this study indicates that a monomeric species was not present.

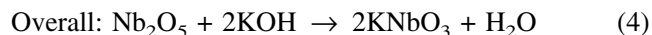
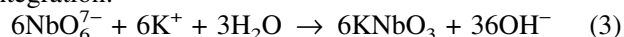
It is proposed that the synthesis of KNbO<sub>3</sub> powders involves the following reactions:



Monomer generation:



Integration:



Reaction (2) is essential since the perovskite structure is composed of corner-sharing NbO<sub>6</sub> octahedra whereas the hexaniobate ion (Nb<sub>6</sub>O<sub>19</sub><sup>8-</sup>) is composed of edge sharing octahedra. As the monomer was not detected in solution by <sup>93</sup>Nb NMR spectroscopy, this suggests that Reaction (2) took place at the surface of a growing crystal instead of in the bulk solution.

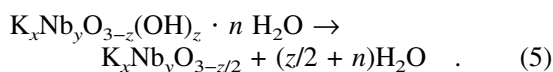
According to Reaction (2), the stability of the hexaniobate ion in KOH solutions decreases with increasing KOH concentrations. This is experimentally supported by the observation that the induction period is shorter for higher KOH concentrations (9 M KOH curve in Fig. 5) in this study, and also by the observation of Lu and Lo<sup>39</sup>

that the mass of KNbO<sub>3</sub> powder recovered after heating a starting solution of KOH and predissolved niobium species at 200 °C increases with increasing KOH concentration for the same processing time.<sup>39</sup> As such, the breakup of the hexaniobate ion according to Reaction (2) is possibly the rate-determining step of the overall reaction. The variation in induction periods also explains the different amounts of recovered powder observed by Kormaneni *et al.*<sup>8</sup> and Lu *et al.*<sup>9</sup> for syntheses in varying KOH concentrations.

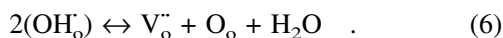
## B. Proton incorporation and removal

Protons may be present in the perovskite lattice either in the form of hydroxyl ions or as H<sub>2</sub>O molecules. The presence of hydroxyl ions in the lattice (residing on sites normally occupied by oxygen atoms) is presumably charge compensated by the presence of cation vacancies, which may lead to A/B cation ratios below one. This type of nonstoichiometry has been observed for hydrothermally synthesized BaTiO<sub>3</sub> and KTaO<sub>3</sub> powders and also for the KNbO<sub>3</sub> powders in this study.<sup>40–42</sup> As for H<sub>2</sub>O molecules, it was proposed in an earlier work that H<sub>2</sub>O molecules reside on vacant potassium sites, based primarily on the similarity in size of K and H<sub>2</sub>O.<sup>42</sup>

The chemical formula of the as-synthesized potassium niobate hydrate may be written as K<sub>x</sub>Nb<sub>y</sub>O<sub>3-z</sub>(OH)<sub>z</sub> · nH<sub>2</sub>O, where  $x + 5y + z = 6$  for charge neutrality. The dehydration reaction that occurs upon heating can, in turn, be written in terms of the overall change in stoichiometry, as shown in Reaction (5):



This dehydration involves both the loss of molecular water and water present in the form of hydroxyl ions, the latter occurring according to<sup>43,44</sup>



The presence of both water and hydroxyl ions in the perovskite lattice, at least for the 6.7 M powder, is supported by NMR observations of two different types of internally incorporated protons (see Fig. 9). The combination of the charge neutrality condition ( $x + 5y + z = 6$ ), weight loss of internally incorporated protons ( $z/2 + n$ ), K/Nb cation ratio ( $x = 0.96y$ ), and requirement that there be just sufficient potassium vacancies to accommodate all water molecules ( $n = 1 - x$ ) leads to a chemical formula of K<sub>0.95</sub>Nb<sub>0.99</sub>O<sub>2.92</sub>(OH)<sub>0.08</sub> · 0.05H<sub>2</sub>O for the 6.7 M powder.

For the KNbO<sub>3</sub> powders studied here, 74% and 38% of the weight loss for the 15 and 6.7 M powders, respectively, occurs below 350 °C. In contrast, the onset of dehydration for barium zirconate, a protonic conductor deliberately doped to produce oxygen vacancies, is reported to take place at temperatures between 350 and

550 °C.<sup>45</sup> The dehydration of KNbO<sub>3</sub> powders at such low temperatures occurs despite the fact that the perovskite structure is a close-packed structure with all oxygen sites in the hydrated perovskite filled with oxygen or hydroxyl ions and all potassium sites filled with potassium ions or water molecules. That is, there is no path for the diffusion of water molecules out of the structure.

To account for the rapid loss of water at low temperatures, it was proposed in our earlier work that the water molecules and hydroxyl ions [via Reaction (6)] at the surface are lost first.<sup>42</sup> This creates vacant sites (potassium and oxygen vacancies) for the subsequent diffusion of water molecules from beneath the surface. This process of vacancy creation proceeds inwards, analogous to a drying front, as water molecules diffuse to the surface. Note that because the water molecule is a neutral species with a Coulombic radius of 1.37 Å,<sup>46</sup> it could diffuse to the surface by hopping through either the vacant potassium sites (radius,  $r = 1.60$  Å)<sup>47</sup> or the vacant oxygen sites ( $r = 1.42$  Å).<sup>47</sup>

## V. CONCLUSIONS

Orthorhombic NaNbO<sub>3</sub> powders were hydrothermally synthesized at 200 °C from 8.4 M NaOH solutions and 0.25 M Nb<sub>2</sub>O<sub>5</sub> powder. For orthorhombic KNbO<sub>3</sub> powders, the reaction was between Nb<sub>2</sub>O<sub>5</sub> (0.0015–0.38 M) and KOH solutions of varying concentrations (6.7–15 M) at 150 and 200 °C. It was observed that an intermediate hexaniobate species formed first before eventually converting to the perovskite phase. For the KOH concentrations studied, most of the Nb<sub>2</sub>O<sub>5</sub> precursor powder dissolved to form a hexaniobate ion, Nb<sub>6</sub>O<sub>19</sub><sup>8-</sup>. The stability of the hexaniobate ion in solution was greater for lower KOH concentration and lower temperature. In other words, the induction period relating to the conversion of the hexaniobate ion to perovskite powder varied with different KOH concentrations for a given temperature. This explains why other studies on hydrothermally synthesized KNbO<sub>3</sub> observed large disparities in the mass of recovered powder for syntheses with varying KOH concentrations. As for the defect structure of the as-synthesized KNbO<sub>3</sub> powder, it was believed that protons were incorporated in the lattice in the form of water molecules and hydroxyl ions, leading to a chemical formula of K<sub>0.95</sub>Nb<sub>0.99</sub>O<sub>2.92</sub>(OH)<sub>0.08</sub> · 0.05H<sub>2</sub>O for the powder synthesized at 200 °C in 6.7 M KOH.

## ACKNOWLEDGMENTS

This work was supported by the Materials Research Laboratory program of the National Science Foundation under Award No. DMR00-80034. G.K.L. Goh acknowledges the Institute of Materials Research and Engineering (Singapore) for the provision of a research scholarship. Dr. Joon Hwan Choi is thanked for the TEM

results while Dr. Sonjong Hwang of the California Institute of Technology is thanked for collecting the <sup>1</sup>H MAS NMR data.

## REFERENCES

1. P. Gunter, *Opt. Commun.* **11**, 285 (1974).
2. Y. Uematsu, *Jpn. J. Appl. Phys.* **13**, 1362 (1974).
3. P. Gunter and F. Micheron, *Ferroelectrics* **18**, 27 (1978).
4. U. Fluckiger, H. Arend, and H.R. Oswald, *J. Am. Ceram. Soc.* **56**, 575 (1977).
5. A. Nazeri-Eshghi, A.X. Kuang, and J.D. Mackenzie, *J. Mater. Sci.* **25**, 3333 (1990).
6. M.M. Amini and M.D. Sacks, *J. Am. Ceram. Soc.* **74**, 53 (1991).
7. M.J. Kim and E. Matijevic, *J. Mater. Res.* **7**, 912 (1992).
8. S. Kormarneni, R. Roy, and Q.H. Li, *Mater. Res. Bull.* **27**, 1393 (1992).
9. C-H. Lu, S-Y. Lo, and H-C. Lin, *Mater. Lett.* **34**, 172 (1998).
10. S. Uchida, Y. Inoue, Y. Fujishiro, and T. Sato, *J. Mater. Sci.* **33**, 5125 (1998).
11. K. Wang, U. Helmersson, S. Olafsson, S. Rudner, L. Wermlund, and S. Gevorgian, *Appl. Phys. Lett.* **73**, 927 (1998).
12. C-R. Cho, J-H. Koh, A. Grishin, S. Abadei, and S. Gevorgian, *Appl. Phys. Lett.* **76**(13), 1761 (2000).
13. H. Schafer, R. Gruehn, and F. Schulte, *Agnew. Chem. Int. Ed.* **5**, 40 (1966).
14. Powder Diffraction File, Card No. 37-1486 (Joint Committee on Powder Diffraction Standards, Swarthmore, PA, 1992).
15. Powder Diffraction File, Card No. 27-1003 (Joint Committee on Powder Diffraction Standards, Swarthmore, PA, 1992).
16. Powder Diffraction File, Card No. 14-0370 (Joint Committee on Powder Diffraction Standards, Swarthmore, PA, 1992).
17. Powder Diffraction File, Card No. 33-1270 (Joint Committee on Powder Diffraction Standards, Swarthmore, PA, 1992).
18. Powder Diffraction File, Card No. 32-0822 (Joint Committee on Powder Diffraction Standards, Swarthmore, PA, 1992).
19. E.A. Wood, *Acta Crystallogr.* **4**, 358 (1951).
20. H.C. Zeng, T.C. Chong, L.C. Lim, H. Kumagai, and M. Hirano, *J. Cryst. Growth* **160**, 289 (1996).
21. G.K.L. Goh, C.G. Levi, J.H. Choi, and F.F. Lange (in press).
22. R.S. Tobias, *Can. J. Chem.* **43**, 1222 (1965).
23. F.J. Farrell, V.A. Maroni, and T.G. Spiro, *Inorg. Chem.* **8**, 2638 (1969).
24. T.J. Boyle, T.M. Alam, D. Dimos, G.J. Moore, C.D. Buchheit, H.N. Al-Shareef, E.R. Mechenbier, B.R. Bear, and J.W. Ziller, *Chem. Mater.* **12**, 3187 (1997).
25. J.A. Gadsen, *Infrared Spectra of Minerals and Related Inorganic Compounds* (Butterworths, London, U.K., 1975), p. 16.
26. V. Augugliaro, S. Coluccia, V. Loddo, L. Marchese, G. Martra, L. Palamisano, and M. Schiavello, *Appl. Catal. B* **20**, 15 (1999).
27. R. B. Barnes, R. C. Gore, U. Liddel, and V. Z. Williams, *Infrared Spectroscopy* (Reinhold, New York, 1944), p. 19.
28. E. Brunner, H.G. Karge, and H. Pfeifer, *Z. Phys. Chem.* **176**, 173 (1992).
29. M. Filowitz, R.K.C. Ho, W.G. Klemperer, and W. Shum, *Inorg. Chem.* **18**(1), 93 (1979).
30. I. Lindqvist, *Arkiv. Kemi.* **5**, 247 (1953).
31. L.C.W. Baker and D.C. Glick, *Chem. Rev.* **98**, 3 (1998).
32. G. Jander and D. Ertel, *J. Inorg. Nucl. Chem.* **14**, 77 (1960).
33. J-M. Jehng and I.E. Wachs, *Chem. Mater.* **3**, 100 (1991).
34. A. Goiffon and B. Spinner, *Rev. Chim. Min.* **11**, 262 (1974).
35. A. Goiffon, R. Granger, C. Bockel, and B. Spinner, *Rev. Chim. Min.* **10**, 487 (1973).
36. W. P. Griffith and T. D. Wickins, *J. Chem. Soc. A* 1087 (1966).
37. *NMR of Newly Accessible Nuclei*, edited by P. Laszlo (Academic Press, New York, 1983), Vol. 2, p. 395.
38. Y-J. Lu, R. Lalancette, and R.H. Beer, *Inorg. Chem.* **35**, 2524 (1996).
39. C-H. Lu and S-Y. Lo, *Ceram. Trans.* **94**, 397 (1999).
40. A.T. Chien, X. Xu, J.H. Kim, J.S. Speck, and F.F. Lange, *J. Mater. Res.* **14**, 3330 (1999).
41. E-W. Shi, C-T. Xia, W-Z. Zhong, B-G. Wang, and C-D. Feng, *J. Am. Ceram. Soc.* **80**, 1567 (1997).
42. G.K.L. Goh, S.M. Haile, C.G. Levi, and F. F. Lange, *J. Mater. Res.* **17**, 3168 (2002).
43. S. Wada, T. Suzuki, and T. Noma, *J. Ceram. Soc. Jpn.* **104**, 383 (1996).
44. D. Hennings and S. Schreinemacher, *J. Eur. Ceram. Soc.* **9**, 41 (1992).
45. K.D. Kreuer, St. Adams, W. Münch, A. Fuchs, U. Klock, and J. Maier, *Solid State Ionics.* **145**, 295 (2001).
46. A-J. Li and R. Nussinov, *Proteins.* **32**, 111 (1998).
47. R.D. Shannon and C.T. Prewitt, *Acta Crystall. B* **25**, 925 (1969).